

## Self-aligned nanostructures created by swift heavy ion irradiation

Hans-Gregor Gehrke,<sup>1,a)</sup> Anne-Katrin Nix,<sup>1</sup> Hans Hofsäss,<sup>1</sup> Johann Krauser,<sup>2</sup> Christina Trautmann,<sup>3</sup> and Alois Weidinger<sup>4</sup>

<sup>1</sup>Physikalisches Institut, Universität Göttingen, Friedrich-Hundplatz 1, D-37077 Göttingen, Germany

<sup>2</sup>Hochschule Harz, Friedrichstraße 57-59, D-38855 Wernigerode, Germany

<sup>3</sup>GSI Helmholtzzentrum für Schwerionenforschung, Planckstr. 1, D-64291 Darmstadt, Germany

<sup>4</sup>Helmholtz-Zentrum Berlin für Materialien und Energie, Hahn-Meitner-Platz 1, D-14109 Berlin, Germany

(Received 15 July 2009; accepted 8 February 2010; published online 6 May 2010)

In tetrahedral amorphous carbon (ta-C) swift heavy ions create conducting tracks of about 8 nm in diameter. To apply these nanowires and implement them into nanodevices, they have to be contacted and gated. In the present work, we demonstrate the fabrication of conducting vertical nanostructures in ta-C together with self-aligned gate electrodes. A multilayer assembly is irradiated with GeV heavy ions and subsequently exposed to several selective etching processes. The samples consist of a Si wafer as substrate covered by a thin ta-C layer. On top is deposited a SiN<sub>x</sub> film for insulation, a Cr layer as electrode, and finally a polycarbonate film as ion track template. Chemical track etching opens nanochannels in the polymer which are self-aligned with the conducting tracks in ta-C because they are produced by the same ions. Through the pores in the polymer template, the Cr and SiN<sub>x</sub> layers are opened by ion beam sputtering and plasma etching, respectively. The resulting structure consists of nanowires embedded in the insulating carbon matrix with a built in gate electrode and has potential application as gated field emission cathode. © 2010 American Institute of Physics. [doi:10.1063/1.3354093]

### I. INTRODUCTION

Ion tracks are created when heavy ions of sufficiently high kinetic energy (usually above 1 MeV per nucleon) pass through solids. The large energy deposition along the ion trajectory causes electronic excitation and ionization processes followed by a rapid temperature spike within a localized cylindrical volume. Depending on the material properties, this temperature increase may cause local melting followed by rapid cooling. In many solids, in particular in insulators, this process freezes in a cylindrical damage zone consisting of defect-rich and otherwise modified material. More complete information on ion track formation in different materials and their properties can be found, e.g., in Refs. 1–6.

Ion tracks have the ideal dimensions for nanotechnology applications. In most materials, their diameter is around 10 nm and their length can be adjusted by the range of the ions, which depends on the beam energy, ion mass, and target composition. Typical ranges of swift heavy ions used in this study are in the order of 10 to 100  $\mu\text{m}$ .<sup>7</sup> If the range is larger than the sample thickness, the ions pass through and are stopped in the substrate or in a beam catcher. It also should be emphasized that the track formation is a single ion effect and therefore does not depend on beam focusing. The created tracks are straight, parallel to each other, and stochastically distributed.

Ion tracks, in particular when combined with chemical etching, provide a powerful tool in nanotechnology. The etching process preferentially dissolves the damaged material of the tracks and enlarges these zones to nanochannels.

Their final diameter can be adjusted by the etching conditions, typically between a few tens of nanometers and several micrometers. Ion track membranes are used as filters with monodisperse channels of controlled size and geometry. Ion track membranes are also successfully utilized as templates, e.g., to grow, metallic nanowires by electrodeposition.<sup>8,9</sup> Furthermore, nanopores can serve as mask for structuring a substrate underneath. This lithographic method has been applied by Bernhardt *et al.*,<sup>10</sup> but has not been developed much since then. In this project, the track technique was implemented during one of the process steps for device structuring.

The central part of the sample is the layer of tetrahedral amorphous carbon (ta-C) also known as diamond-like carbon (DLC). It has been demonstrated that each swift heavy ion converts this insulator into a graphitic nanowire of about 8 nm in diameter.<sup>6,11</sup> Figure 1 shows an atomic force microscopy (AFM) image recorded using a conducting AFM tip and measuring the current between the Si substrate (back contact) and the surface of an irradiated ta-C film.

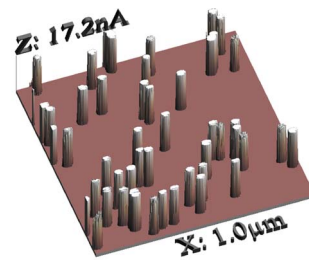


FIG. 1. (Color online) Presentation of a two dimensional AFM scan recording the current distribution over an area of 1  $\mu\text{m}^2$  between an AFM tip and the back contact of a 100 nm thick ta-C film irradiated with 1-GeV U ions at a fluence of  $5 \times 10^9$  ions/cm<sup>2</sup>. By passing through ta-C each ion converts the insulating ta-C along the path into conducting graphite-like carbon Ref. 6.

<sup>a)</sup>Electronic mail: hgehrke1@gwdg.de.

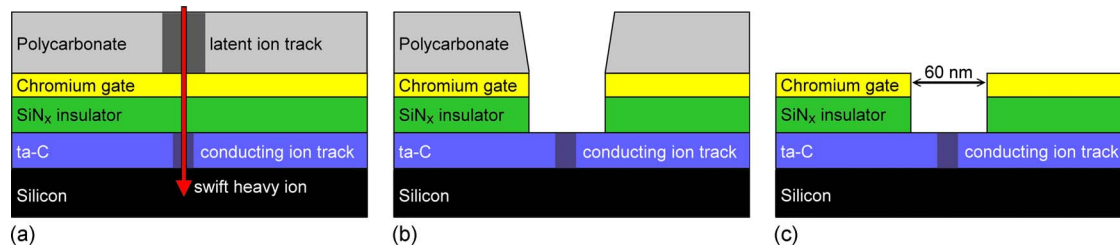


FIG. 2. (Color online) Schematics of the production of the nanodevice. (a) Irradiation of multilayer stack consisting of ta-C (75 nm) on Si wafer with SiN<sub>x</sub> (45–110 nm), Cr (40 nm), and polycarbonate (600 nm) on top. 1-GeV U ions produce tracks in polycarbonate and ta-C. (b) Selective etching and ion beam sputtering opens access to the ta-C layer. (c) Final structure.

The current increases by 3–4 orders of magnitude when the tip is in contact with an ion track. The conductance increase is ascribed to the conversion of the material along the ion path from insulating diamond-like ( $sp^3$  hybridization rich coordination) to conducting graphite-like ( $sp^2$  hybridization rich coordination) carbon. In the presented nanostructure, this conducting track acts as a thin nanowire-like contact.

The structure presented here is similar to that reported in Ref. 10 but the dimensions are more than five times smaller and the conducting track in ta-C replaces the field emission cones (*Spindt tips*<sup>12</sup>), which are difficult to fabricate. We expect that the narrower geometry in our case can compensate the less favorable emission behavior of embedded wires compared to the field emission cones in Ref. 10 but this remains to be shown.

## II. EXPERIMENTAL

The sample consists of four different layers (see Fig. 2) deposited on a highly n-type doped Si substrate ( $5 \times 10^{-4} \Omega \text{ cm}$ ). The first layer is a 75 nm thick ta-C layer created by implementation of mass-selected 100 eV carbon ions.<sup>13</sup> It follows an insulating nonstoichiometric SiN<sub>x</sub> layer produced at the Helmholtz Centre Berlin by plasma enhanced chemical vapor deposition (PECVD) at 300 °C. The plasma gas consists of a mixture of SiH<sub>4</sub>, NH<sub>3</sub>, and N<sub>2</sub> with fluxes in the ratio 1:6:2 and a total pressure of 43 Pa. The average deposition rate was 7.4 nm/min. In the present experiment we chose thicknesses between 45 and 110 nm. The third layer consists of a 40 nm thick evaporated Cr film serving as electrode. Finally, a 600 nm polycarbonate layer is spin-coated onto the Cr film.<sup>14</sup>

The entire multilayer stack was irradiated with swift heavy ions at the GSI Helmholtz Centre in Darmstadt. Typically, we use U ions of about 1 GeV energy, but somewhat lighter and less energetic ions (e.g., 140 MeV Xe ions), are also suitable. At such energies, the ion range is sufficiently large to pass easily through all four layers. They are implanted far inside the Si substrate [depth approximately 50  $\mu\text{m}$  Ref. 7)]. To minimize track overlapping, we choose fluences between  $10^8$  and  $10^9$  ions/cm<sup>2</sup> depending on the analysis technique applied afterwards. These fluences correspond to 1 and 10 (stochastically distributed) ion tracks on an area of 1  $\mu\text{m}^2$ . To achieve access to the lower layers and contact the track in the ta-C layer, the irradiated sample is selectively etched and processed by different methods.

In a first step, the polymer is etched in a 5 molar NaOH solution for about 45 min at room temperature. This treatment attacks the ion tracks in the polymer and creates channels through-going to the Cr layer as demonstrated in an earlier experiment.<sup>14</sup>

Figure 3 shows a scanning electron microscopy (SEM) image of the surface of the etched polymer layer with channels of 50–60 nm diameter. At a pore density of  $10^9 \text{ cm}^{-2}$ , the open surface area is about 2.8%, leading to occasional overlapping of the openings which is neglectable for practical purposes. However, if this is a problem or in case larger pores are required, overlapping could be avoided by applying smaller irradiation fluences.

Opening the Cr and SiN<sub>x</sub> layers was achieved by sputtering with mass selected Ar ions of fluences in the order of several  $10^{17}$  ions/cm<sup>2</sup> and energies of 15, 5, and 1 keV. In order to minimize intermixing at the bottom of the insulator film, lower energies were applied as the holes get deeper. Finally, polycarbonate is removed in concentrated dichloromethane. The pores of the Cr layer now serve as aperture for completely opening the SiN<sub>x</sub> by plasma etching. This process was performed at the Technical University of Berlin in a commercial set up (Oxford Plasmalab 80 Plus) using an oxygen free gas mixture of CHF<sub>3</sub> [25 SCCM (SCCM denotes cubic centimeter per minute at STP)] and Ar (25 SCCM) at a pressure of 3750 Pa and at a temperature of 288 K. The etching time was 6 min at a power of 150 W.

For cross section imaging, the resulting multilayer sys-

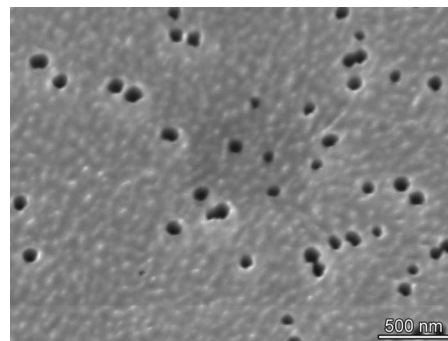


FIG. 3. SEM image of polycarbonate film irradiated with 1-GeV U ions of fluence of  $1 \times 10^9$  ions/cm<sup>2</sup> and track etched in 5 mol/l NaOH for 45 min at room temperature. The resulting nanochannels have a diameter of about 50–60 nm, their density corresponds to the irradiation fluence. To avoid sample charging during SEM imaging, the sample was sputter-coated by a 5–10 nm gold layer.

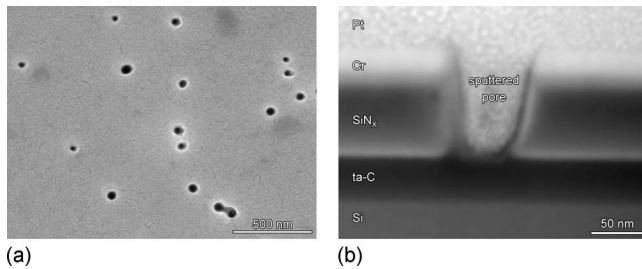


FIG. 4. (a) SEM image of Cr surface after removal of polycarbonate resist serving as template for the sputtering process. The holes in the Cr layer are replica of the track etched pores in the resist. (b) Cross section SEM image of the pores. For the highest sputtering fluence chosen here ( $1.03 \times 10^{18}$  ions/cm<sup>2</sup>), the holes go through the Cr and SiN<sub>x</sub> film and reach the ta-C layer. The cross section was imaged under a tilt angle of 53° after depositing a Pt layer for sample stabilization and subsequent cutting a trench into the sample by FIB.

tem was cut normal to the surface by focused ion beam (FIB). To stabilize the structure during FIB treatment, a 1–2 μm Pt layer was deposited *in situ* in a two-step process over an area of a few micrometer square. The first 200 nm were created by electron beam induced deposition. The remainder was deposited by ion beam induced deposition. This preparation allows a smooth and perpendicular wedge-shaped cut through the layers of interest.

In order to test the suitability of the Cr layer as gate electrode, the current transport of a 0.25 mm wide, 3 mm long, and 40 nm thick Cr pad was measured. The resistance of this Cr structure is 760 Ω, while the resistance of the SiN<sub>x</sub> insulator between Cr pad and the substrate is larger than 400 kΩ. Although the conductivity of this Cr layer (400 kS/m) is reduced compared to bulk material, it is still sufficiently large with respect to the resistance of the insulator. No mentionable voltage drop along a chromium pad is expected.

### III. RESULTS AND DISCUSSION

#### A. Argon ion sputtering

Since ion tracks are not formed in Cr, this layer was opened by Ar ion beam sputtering using the pores in the polycarbonate film as template. The low angular divergence of this beam allowed sputter erosion through a pore with an aspect ratio larger than 10:1. SEM images of the Cr surface clearly show holes in the Cr layer [Fig. 4(a)]. The number of the holes and their diameters are in agreement with the nanochannels in the polycarbonate template. The agreement of the diameter suggests cylindrical pores in the polycarbonate film. Ar ion sputtering is obviously an adequate method to transfer nanopores from the resist to the layers below. The resulting depth of the holes in the Cr-layer and SiN<sub>x</sub>-layer depends primarily on the fluence of the sputtering ion (see Table I) and can reach down to the ta-C layer. We found that the diameter of the pores in the Cr electrode is independent of the sputter fluence within the range covered by Table I. The average pore diameters are again 50 to 60 nm, i.e., the same as in polycarbonate.

Table I summarizes the results of the Ar ion sputtering treatment. For calculating the depth of the holes, the specific

TABLE I. Pore depths under Ar ion sputtering with four different fluences ( $\Phi$ ) as calculated using the stopping and range of ions in matter (SRIM-2006.02 code) (Ref. 7) and deduced from cross section SEM images.

$\Phi$ ( $10^{17}$ ions/cm <sup>2</sup> )	Calculated depth (nm)	Measured depth (nm)	Depth ratio (measured/calculated)
2.86	80	50	0.63
4.80	120	80	0.67
8.29	190	110	0.58
10.32	300	170	0.57

sputter yields of different materials and energies were taken into account. The results show that sputtering through 60 nm wide and 600 nm long polycarbonate channels is possible, though the sputtering rate is reduced to about 60% compared to calculated values on free surfaces. The reduction seems to be reasonable considering redeposition of material during sputtering and scattering of the sputter ions. An advantage of this process is that the sputtering depth can practically be controlled independently from the pore diameter of the mask.

#### B. Plasma etching

Although it is possible to open the channels through the SiN<sub>x</sub> layer by Ar sputtering as demonstrated in Fig. 4(b), it was tried to complete the drilling process by an alternative selective etching process. The main reasons for this measure are unwanted intermixing caused by sputtering and the risk of changing the  $sp^2$  and  $sp^3$  hybridization at the surface of the ta-C layer. Since the polymer decomposes during the plasma etching process applied for the SiN<sub>x</sub> layer, the polymer could not serve as mask, but the pores in the Cr film had to be used instead. For a soft pore opening procedure, ion beam sputtering was thus limited to low fluences ( $4.8 \times 10^{17}$  ions/cm<sup>2</sup>) leaving sufficient SiN<sub>x</sub> intact. Then the polycarbonate film was removed in dichloromethane and plasma etching was applied. Figure 5 shows a pore before and after this plasma treatment. Figure 5(a) illustrates that under the applied sputtering condition, the Ar beam produces a through-going pore in the Cr layer, but also slightly opens the SiN<sub>x</sub> layer. By the subsequent plasma etching process [Fig. 5(b)], only the SiN<sub>x</sub> pore is opened giving access to the track in the ta-C layer. The selectivity of the procedure was checked by etching a large area of SiN<sub>x</sub> on top of a ta-C film

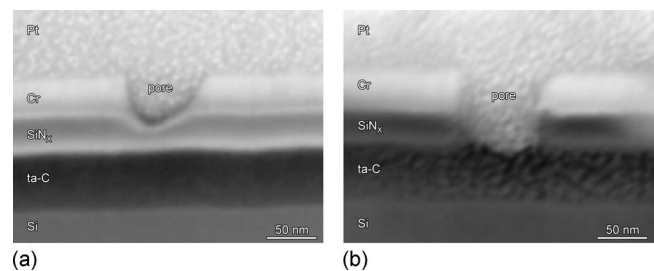


FIG. 5. Cross section images of pores pretreated by sputtering with  $4.8 \times 10^{17}$  cm<sup>-2</sup> Ar ions before (a) and after (b) plasma treatment. Ar sputtering produced a hole in the Cr layer and slightly entered into the SiN<sub>x</sub> layer, subsequent plasma etching selectively opens the SiN<sub>x</sub> layer giving access to the track in the ta-C layer (dark layer).

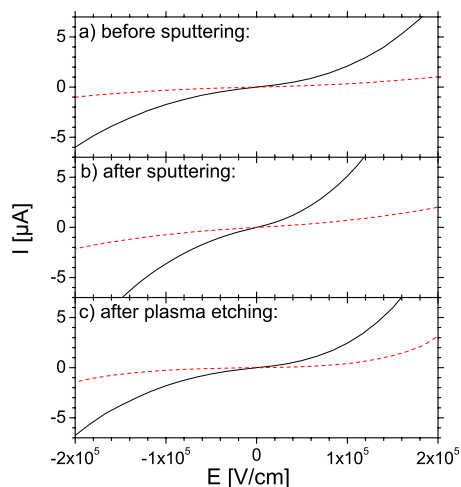


FIG. 6. (Color online) Electrical current between a Cr contact pad and the conducting Si substrate as a function of electrical field (applied voltage normalized by stack thickness). Solid and dashed lines represent measurements on two different contact pads. (a) after ion irradiation, (b) after Ar ion sputtering, and (c) after subsequent plasma etching. The  $\text{SiN}_x$  layer thickness was 100 nm (a and b) and 60 nm (c). The selected Cr contacts in (a) and (b) are the same, the measurements in (c) were made on different contacts.

as described above. The film thickness of the ta-C was measured before and after the etching and revealed no significant change. Thus, the process does not attach the ta-C film, but completely removes the 70 nm  $\text{SiN}_x$  layer.

### C. Electrical measurements

Figure 6 shows the current versus electrical-field curves of the multilayer stack before and after the sputtering and plasma etching processes for two different Cr contact pads. The current measurements slightly differ for the two selected contacts and exhibit some additional leakage current after the sputtering and plasma etching treatments, but these deteriorations remain moderate. The present arrangement withstood electrical fields up to about 0.4 MV/cm between the Cr electrode and the Si substrate. For field emission applications, it is planned to improve the stability against breakthrough by preparing the layers under more controlled conditions (occasional weak points in the insulator are probably the reason for the breakthrough). In the literature, PECVD-produced  $\text{SiN}_x$  layers are reported to have a breakthrough stability better than 10 MV/cm.<sup>15</sup> The present experiment shows the feasibility of the various structuring processes, but the electrical properties of the layers, in particular of the insulator, are not yet optimized.

### IV. CONCLUSION

This study presents a novel multistep approach to contact conducting ion tracks in ta-Ca films. For device control and application, the ta-C film is covered by several layers

composed of metallic Cr as electrode, insulating  $\text{SiN}_x$ , and polymer resist as mask. By exposing the multilayer sample to high-energy heavy particles, cylindrical ion tracks are produced in the insulating layers but not in Cr. Tracks in ta-C are conducting and have a diameter of about 8 nm. To integrate them as nanowires in more complex nanoelectronic devices, narrow apertures (50–80 nm) were produced by selectively opening access to the ta-C tracks through the different layers of the stack. The proposed procedure is a self-aligned process and involves chemical track etching of the polymer resist, followed by ion sputtering of the Cr through the pores of the polymer mask. This process step is beam parameter controlled providing a depth precision of a few nanometers. Finally it is demonstrated that plasma etching is selective enough to remove the  $\text{SiN}_x$  layer through the apertures in the Cr layer giving direct access to the conducting ta-C tracks.

### ACKNOWLEDGMENTS

We would like to thank Dr. Peter-Joachim Wilbrandt, Mathias Hahn, and Volker Radisch from the Institute of Material Physics Göttingen, Germany for their help regarding the FIB preparations. We thank also Dr. Frank Wunsch from the Helmholtz-Zentrum Berlin for preparing the  $\text{SiN}_x$  layers and Dr. Jürgen Bruns from the Technische Universität Berlin for performing the plasma etching. The work is financially supported by the DFG (Grant No. Ho1125/17-1) and BMBF (Grant No. 05 KK4MGA/9)

<sup>1</sup>E. Ferain and R. Legras, *Nucl. Instrum. Methods Phys. Res. B* **174**, 116 (2001).

<sup>2</sup>A. Adla, H. Fuess, and C. Trautmann, *J. Polym. Sci., Part B: Polym. Phys.* **41**, 2892 (2003).

<sup>3</sup>M. Toulemonde, C. Trautmann, E. Balanzat, K. Hjort, and A. Weidinger, *Nucl. Instrum. Methods Phys. Res. B* **216**, 1 (2004).

<sup>4</sup>M. Toulemonde, W. Assmann, C. Dufour, A. Meftah, F. Studer, and C. Trautmann, *The Royal Danish Academy of Science and Letters* **376**, 384 (2006).

<sup>5</sup>A. Dallanora, T. L. Marcondes, G. G. Bermudez, P. F. P. Fichtner, C. Trautmann, M. Toulemonde, and R. M. Papaleo, *J. Appl. Phys.* **104**, 024307 (2008).

<sup>6</sup>J. Krauser, J.-H. Zollondz, A. Weidinger, and C. Trautmann, *J. Appl. Phys.* **94**, 1959 (2003).

<sup>7</sup>J. Ziegler, <http://www.srim.org/>, 2008.

<sup>8</sup>M. E. T. Molaes, E. M. Hohberger, Ch. Schaefflein, R. H. Blick, R. Neumann, and C. Trautmann, *Appl. Phys. Lett.* **82**, 2139 (2003).

<sup>9</sup>L. Gravier, J.-E. Wegrowe, T. Wade, A. Fabian, and J.-P. Ansermet, *IEEE Trans. Magn.* **38**, 2700 (2002).

<sup>10</sup>A. F. Bernhardt, R. J. Contolini, A. F. Jankowski, V. Liberman, J. D. Morse, R. G. Musket, R. Barton, J. Macaulay, and C. Spindt, *J. Vac. Sci. Technol. B* **18**, 1212 (2000).

<sup>11</sup>M. Waiblinger, Ch. Sommerhalter, B. Pietzak, J. Krauser, B. Mertesacker, M. Ch. Lux-Steiner, S. Klumppner, A. Weidinger, C. Ronning, and H. Hofsäss, *Appl. Phys. A: Mater. Sci. Process.* **69**, 239 (1999).

<sup>12</sup>C. A. Spindt, *J. Appl. Phys.* **39**, 3504 (1968).

<sup>13</sup>H. Hofsäss, H. Binder, T. Klumpp, and E. Recknagel, *Diamond Relat. Mater.* **3**, 137 (1994).

<sup>14</sup>A.-K. Nix, H.-G. Gehrke, J. Krauser, C. Trautmann, A. Weidinger, and H. Hofsäss, *Nucl. Instrum. Methods Phys. Res. B* **267**, 1032 (2009).

<sup>15</sup>Y. Manabe and T. Mitsuyu, *J. Appl. Phys.* **66**, 2475 (1989).